Available online at www.sciencedirect.com
ScienceDirect
Mechanics Research Communications 34 (2007) 553–560
MECHANICS RESEARCH COMMUNICATIONS
www.elsevier.com/locate/mechrescom

Thermoelastic coupled modeling for a thermal bimorph actuator

Liang-Chieh Wu [a], Kow-Ming Chang [b,*]

[a] Department of Mechanical Engineering, National Taiwan University, No. 1, Sec. 4, Roosevelt Road, Taipei 10617, Taiwan
[b] Department of Electronics Engineering, National Chiao Tung University, 1001 Ta Hsueh Road, Hsinchu 30010, Taiwan

Received 10 January 2007; received in revised form 20 July 2007
Available online 10 August 2007

Abstract

This paper presents a theoretical thermoelastic coupled model for a thermal bimorph actuator driven by a harmonically varying thermal load in micro-electro-mechanical systems. The thermoelastic coupling, which arises from the coupling of the strain rate to the temperature field of the heat transport, is considered in this model. The frequency responses are simulated using the theorem of eigenmode expansion. The effects of thermoelastic coupling on the resonant frequency and the quality factor Q for each eigenmode resonance of the deflection are calculated and compared with the same effects resulted from air damping. It shows that for the example of an aluminum–polysilicon thermal bimorph actuator, the resonant frequencies are generally shifted downward with the order larger than that of air damping, whereas the influence of thermoelastic coupling on the Q is more significant than that of air damping under high vacuum level.

Keywords: Thermal bimorph actuator; Thermoelastic coupling; Eigenmode expansion; Quality factor

1. Introduction

Among the microactuators' actuation mechanisms, thermal-mechanical technique has been demonstrated with the main advantages of high output force, low driving voltage and simple fabrication processes in micro-electro-mechanical systems (MEMS). The thermo-mechanical behavior of a thermal actuator is a multiphysics phenomenon in which the heat transport and the elastic deformation are field-coupled. The thermoelastic coupling produces an irreversible process in which heat flow is generated by the coupling of the strain rate of the deformed body to the temperature field. This process further brings the loss of energy and the final state of thermal equilibrium (Roszhart, 1990). The resultant energy dissipation is known as the thermoelastic damping. In the MEMS thermal actuator regime, although several modelings for the thermo-mechanical behaviors of the thermal actuators have been proposed, the influences of the thermoelastic coupling are usually ignored. Finite element analysis (FEA) taking into account the modes of heat transfer and the

* Corresponding author. Tel./fax: +886 3 5731887.
E-mail address: kmchang@cc.nctu.edu.tw (K.-M. Chang).

0093-6413/$ - see front matter © 2007 Elsevier Ltd. All rights reserved.
doi:10.1016/j.mechrescom.2007.07.005

temperature dependence of thermo-mechanical properties were proposed for the steady-state behavior of the thermal actuators (Mankame and Ananthasuresh, 2001). The dynamic responses of a hot/cold arm thermal actuator and a chevron actuator have also been investigated using transient FEA (Geisberger et al., 2003). Hickey et al. (2003) have presented a lumped model for thermal actuators in which the system parameters could be obtained by the experimental results. Despite there are many developed methods of FEA modeling and lumped model been reported, an analytical model which can give explicit direct relationships among the input and output parameters, physical properties and geometrical parameters, is still a more straightforward and efficient way to evaluate the performance of a thermal actuator. In addition, the issue of thermoelastic damping is mostly concerned for achieving high quality factor Q in the development of microresonators (Yasumura et al., 2000). In this case, the analytical model presented by Zener (1937, 1938) is commonly employed to predict the Q of the beam resonator under the influence of thermoelastic damping. This model is based on the assumption that the heat conduction is in the vertical direction of the beam thickness and thermally isolated from the external medium. In most of the practical thermal bimorph actuators, however, the heat conduction is in the longitudinal direction of the beam length. Therefore, a different approach to characterize the thermoelastic damping of a thermal bimorph actuator is needed.

In this paper, a theoretical model for a thermal bimorph actuator taking into account the thermoelastic coupling is developed. The dynamic responses for a harmonically varying thermal load are simulated using the eigenmode expansion method. By calculating the complex eigenfrequencies of the freely vibrating thermal actuator, the effects of thermoelastic coupling on the resonant frequency and the Q are studied for each eigenmode resonance of the deflection. The calculated thermoelastic damping effects are also compared to the air damping which is generally considered the predominant damping source in the actuation of microstructures.

2. Coupled dynamic model

A thermal bimorph actuator with geometric dimensions of length l, width b, and thickness of h_1 and h_2 for the bimorph layers is shown in Fig. 1. The comprising materials of each layer are assumed homogeneous and isotropic and are denoted by subscripts 1 and 2, respectively. The coordinate system of the beam is defined such that the x-axis is the neutral axis along the longitudinal direction and the z-axis along the beam thickness direction.

The governing equation of such a thermally actuated bimorph cantilever beam with flexural deflection in the z-axis is thus expressed in the following form (Boley and Weiner, 1960):

$$\frac{\partial^2}{\partial^2 x}\left[E_c I_c \frac{\partial^2 w(x,t)}{\partial x^2}\right] + m_c \frac{\partial^2 w(x,t)}{\partial t^2} = \frac{\partial^2 M_T}{\partial x^2}, \tag{1}$$

where t is the time, $E_c I_c$ is the bending modulus, w is the flexural deflection, m_c is the mass of cross-section, and M_T is the thermal moment causing the thermal actuation. Here subscript c denotes the properties of bimorph structure and $E_c I_c$ and m_c can be expressed as

$$E_c I_c = \frac{b\{E_1[(h_0+h_1)^3 - h_0^3] - E_2[h_0^3 - (h_0-h_2)^3]\}}{3}, \quad m_c = b(h_1\rho_1 + h_2\rho_2), \tag{2}$$

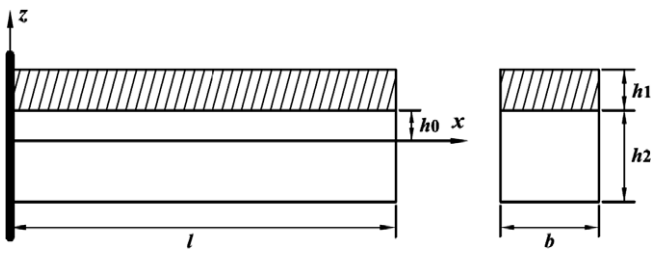

Fig. 1. Schematic diagrams of a thermal bimorph actuator.

where h_0 is the distance from the neutral axis to the interface between materials 1 and 2, E_1, E_2 and ρ_1 and ρ_2 are Young's moduli and the densities of mass, respectively. From the zero resultant force in the cross-section due to the bending strain, the location of the neutral axis can be determined as

$$h_0 = \frac{E_2 h_2^2 - E_1 h_1^2}{2(E_1 h_1 + E_2 h_2)}. \tag{3}$$

The thermal moment in Eq. (1) can be expressed as

$$M_T = \int_{A_1} z\alpha_1 E_1 \theta(x,t)\mathrm{d}A + \int_{A_2} z\alpha_2 E_2 \theta(x,t)\mathrm{d}A = \left[b\frac{E_1 E_2 h_1 h_2 (h_1+h_2)(\alpha_1-\alpha_2)}{2(E_1 h_1 + E_2 h_2)}\right]\theta(x,t) = \beta\theta(x,t), \tag{4}$$

where A_1 and A_2 are the cross-sections, α_1 and α_2 are the coefficients of thermal expansion and $\theta(x,t)$ is the one-dimensional temperature variation from the initial reference temperature T_0. The temperature variation is governed by the heat conduction equation as (Fung, 1965)

$$k\frac{\partial^2\theta}{\partial x^2} + q = \rho c\frac{\partial\theta}{\partial t} + (3\lambda + 2\mu)\alpha T_0 \frac{\partial^2 u}{\partial x \partial t}, \tag{5}$$

where k is the thermal conductivity, q is the internal heat load per unit volume, c is the specific heat at constant deformation, λ and μ are the Lame constants and u is the longitudinal displacement of the beam. Note that the last term in the right hand side of Eq. (5) appears as the thermoelastic coupling term.

The longitudinal normal strain $\frac{\partial u}{\partial x}$ is contributed from two parts: the bending component $-z\frac{\mathrm{d}^2 w}{\mathrm{d}x^2}$ and the average strain ε_0 due to the mismatch of thermal expansion in the longitudinal direction. The average strain can be further obtained from the zero resultant force in the longitudinal direction. Therefore

$$\frac{\partial u}{\partial x} = -z\frac{\mathrm{d}^2 w}{\mathrm{d}x^2} + \varepsilon_0, \quad \varepsilon_0 = \frac{(\alpha_1 E_1 h_1 + \alpha_2 E_2 h_2)}{E_1 h_1 + E_2 h_2}\theta. \tag{6a, b}$$

Substituting Eq. (6a) into Eq. (5) and combining with Eq. (6b), Eq. (5) is further integrated over the beam cross-section, such that

$$k_c\frac{\partial^2\theta}{\partial x^2} + q = \rho_c c_c\frac{\partial\theta}{\partial t} + \kappa_1\frac{\partial\theta}{\partial t} - \kappa_2\frac{\partial^3 w}{\partial x^2 \partial t}, \tag{7}$$

where

$$\begin{aligned} k_c &= \frac{k_1 h_1 + k_2 h_2}{h_1 + h_2}, \quad \rho_c c_c = \frac{\rho_1 c_1 h_1 + \rho_2 c_2 h_2}{h_1 + h_2}, \\ \kappa_1 &= \frac{(\alpha_1 E_1 h_1 + \alpha_2 E_2 h_2)[(3\lambda_1 + 2\mu_1)\alpha_1 T_0 h_1 + (3\lambda_2 + 2\ \mu_2)\alpha_2 T_0 h_2]}{(h_1 + h_2)(E_1 h_1 + E_2 h_2)}, \\ \kappa_2 &= (3\lambda_1 + 2\mu_1)\alpha_1 T_0\left[\frac{(h_0 + h_1)^2 - h_0^2}{2(h_1 + h_2)}\right] + (3\lambda_2 + 2\mu_2)\alpha_2 T_0\left[\frac{h_0^2 - (h_0 - h_2)^2}{2(h_1 + h_2)}\right]. \end{aligned} \tag{8}$$

The deflection w must satisfy the boundary conditions at the clamped and free ends ($x = 0, l$) of the cantilever beam as $w|_{x=0} = 0$, $\frac{\partial w}{\partial x}\big|_{x=0} = 0$, $\frac{\partial^2 w}{\partial x^2}\Big|_{x=l} = 0$ and $\frac{\partial^3 w}{\partial x^3}\Big|_{x=l} = 0$. The cantilever beam is normally clamped to the substrate whose thermal mass is much larger than that of the beam. Therefore the thermal characteristic of the substrate can be considered as an ideal heat sink, and the clamped end of the beam is held at the initial reference temperature throughout actuation as $\theta|_{x=0} = 0$. The free end of the beam is exposed to surrounding air, thus thermal boundary condition here is assumed to be thermally insulated due to relatively low thermal conductivity of air compared to that of the structure materials (Hickey et al., 2003), such that $\frac{\partial\theta}{\partial x}\big|_{x=l} = 0$.

3. Solution

For the problem solving convenience, the dimensionless quantities are introduced as follows:

$$\xi = x/l, \quad \bar{w} = w/l, \quad \tau = \omega_0 t, \quad \bar{\theta} = \theta/T_0, \quad \bar{q} = \frac{l^2 q}{k_c T_0}, \tag{9}$$

where ω_0 is the reference frequency. The coupled governing equations of thermal actuator, Eqs. (1) and (7), in dimensionless form respectively become

$$B_1\frac{\partial^4\bar{w}}{\partial\xi^4}+B_2\omega_0^2\frac{\partial^2\bar{w}}{\partial\tau^2}=B_3\frac{\partial^2\bar{\theta}}{\partial\xi^2},\quad \frac{\partial^2\bar{\theta}}{\partial\xi^2}+\bar{q}=(P_1+P_2)\frac{\partial\bar{\theta}}{\partial\tau}-P_3\frac{\partial^3\bar{w}}{\partial\xi^2\partial\tau}, \tag{10a, b}$$

where

$$B_1=\frac{E_cI_c}{l},\quad B_2=m_cl^3,\quad B_3=\beta T_0,\quad P_1=\frac{\rho_cc_cl^2\omega_0}{k_c},\quad P_2=\frac{\kappa_1l^2\omega_0}{k_c},\quad P_3=\frac{\kappa_2l\omega_0}{k_cT_0}. \tag{11}$$

The boundary conditions of $\bar{w}$ and $\bar{\theta}$ are $\bar{w}|_{\xi=0}=0$, $\left.\frac{\partial\bar{w}}{\partial\xi}\right|_{\xi=0}=0$, $\left.\frac{\partial^2\bar{w}}{\partial\xi^2}\right|_{\xi=1}=0$, $\left.\frac{\partial^3\bar{w}}{\partial\xi^3}\right|_{\xi=1}=0$, $\bar{\theta}|_{\xi=0}=0$ and $\left.\frac{\partial\bar{\theta}}{\partial\xi}\right|_{\xi=1}=0$.

When the thermal actuator is subjected to a harmonically varying thermal load with the dimensionless frequency Ω as $\bar{q}=q^*e^{i\Omega\tau}$, $\bar{w}$ and $\bar{\theta}$ are also harmonically varying due to the linearity of the thermoelastic problem, such that $\bar{w}(\xi,\tau)=w^*(\xi)e^{i\Omega\tau}$ and $\bar{\theta}(\xi,\tau)=\theta^*(\xi)e^{i\Omega\tau}$. Here w^* can be further expanded by an infinite complete set of eigenmodes of an undamped freely vibrating cantilever beam as $w^*=\sum_{n=1}^{\infty}p_n\varphi_n(\xi)$, where p_n and φ_n are the nth undetermined coefficient and the nth eigenmode which satisfies the same boundary conditions as $\bar{w}$. The eigenmode φ_n also satisfies the orthogonal relations in dimensionless coordinate ξ (Melrovitch, 1986) as

$$\int_0^1 B_1\varphi_m\frac{d^4\varphi_n}{d\xi^4}d\xi=\omega_m^2\delta_{mn},\quad \int_0^1 B_2\varphi_m\varphi_n d\xi=\delta_{mn},\quad (m,n=1,2,\ldots), \tag{12a, b}$$

where δ_{mn} is Kronecker delta and ω_m is the natural frequency of the cantilever beam. Using the harmonic forms of $\bar{q}$, $\bar{w}$ and $\bar{\theta}$ and the eigenmode expansion of w^*, Eq. (10) gives

$$B_1\sum_{n=1}^{\infty}p_n\frac{d^4\varphi_n}{d\xi^4}-B_2\Omega^2\omega_0^2\sum_{n=1}^{\infty}p_n\varphi_n=B_3\frac{d^2\theta^*}{d\xi^2},\quad \frac{d^2\theta^*}{d\xi^2}+q^*=i\Omega(P_1+P_2)\theta^*-i\Omega P_3\sum_{n=1}^{\infty}p_n\frac{d^2\varphi_n}{d\xi^2}. \tag{13a, b}$$

From Eq. (13b), the solution of θ^* can be obtained as

$$\theta^*=a_1e^{r_1\xi}+a_2e^{-r_1\xi}-\frac{iq^*}{\Omega(P_1+P_2\eta)}+\frac{P_3}{P_1+P_2}\sum_{n=1}^{\infty}p_n\frac{d^2\varphi_n}{d\xi^2}, \tag{14}$$

where $r_1=\sqrt{i\Omega(P_1+P_2)}$ and a_1 and a_2 are two undetermined coefficients.

Substituting Eq. (14) into Eq. (13a), multiplying Eq. (13a) by $\varphi_m(m=1,2,\ldots)$ and integrating it over the interval $0\leqslant\xi\leqslant1$, an infinite set of equations can be generated. These equations can be further simplified using the orthogonal relations of Eq. (12). Furthermore, two thermal boundary conditions of $\bar{\theta}$ are applied to θ^* in Eq. (14). These coupled equations can be combined and written in a matrix form as $\mathbf{WC}=\mathbf{F}$, where

$$\mathbf{W}=\begin{bmatrix}\omega_1^2-\omega_0^2\Omega^2+H_{11} & 0 & \cdots & 0 & K_{11} & K_{21}\\ 0 & \omega_2^2-\omega_0^2\Omega^2+H_{22} & \cdots & \vdots & K_{12} & K_{22}\\ \vdots & \vdots & \ddots & 0 & \vdots & \vdots\\ 0 & 0 & \cdots & \omega_m^2-\omega_0^2\Omega^2+H_{mm} & K_{1m} & K_{2m}\\ M_1 & M_2 & \cdots & M_m & r_1e^{r_1} & -r_1e^{-r_1}\\ N_1 & N_2 & \cdots & N_m & 1 & 1\end{bmatrix}, \tag{15}$$

$$\mathbf{C}=[p_1\quad p_2\quad\cdots\quad p_m\quad a_1\quad a_2]^T,\quad \mathbf{F}=\left[0\quad\cdots\quad 0\quad \frac{iq^*}{\Omega(P_1+P_2)}\right]^T, \tag{16}$$

with

$$H_{mn} = -\frac{P_3}{(P_1+P_2)}\int_0^1 \varphi_m \frac{\mathrm{d}^4\varphi_n}{\mathrm{d}\xi^4}\mathrm{d}\xi = -\frac{P_3}{(P_1+P_2)B_1}\omega_m^2\delta_{mn}, \quad K_{1m} = -B_3 r_1^2\int_0^1 \varphi_m \mathrm{e}^{r_1\xi}\mathrm{d}\xi, \tag{17}$$

$$K_{2m} = -B_3 r_1^2\int_0^1 \varphi_m \mathrm{e}^{-r_1\xi}\mathrm{d}\xi, \quad M_m = \frac{P_3}{(P_1+P_2)}\left.\frac{\mathrm{d}^3\varphi_m}{\mathrm{d}\xi^3}\right|_{\xi=1}, \quad N_m = \frac{P_3}{(P_1+P_2)}\left.\frac{\mathrm{d}^2\varphi_m}{\mathrm{d}\xi^2}\right|_{\xi=0}. \tag{18}$$

By solving $\mathbf{WC} = \mathbf{F}$, the coupled responses of the temperature and deflection can be determined.

When the thermoelastic coupling term in Eq. (13b) is not taken into account, the coupled problem is separated into two problems which can be solved consecutively. The first to be solved is the problem of conventional heat conduction. The uncoupled dimensionless temperature satisfying the thermal boundary conditions of $\bar{\theta}$ can then be obtained as

$$\theta^* = \frac{\mathrm{i}q^*(\mathrm{e}^{r_2\xi} + \mathrm{e}^{2r_2 - r_2\xi} - \mathrm{e}^{2r_2} - 1)}{\Omega P_1(\mathrm{e}^{2r_2}+1)}, \tag{19}$$

where $r_2 = \sqrt{\mathrm{i}\Omega P_1}$. Substituting Eq. (19) into Eq. (13a), the calculated temperature can be seen as an external load to the cantilever. By multiplying Eq. (13a) with $\varphi_m (m = 1,2,\ldots)$, integrating it over the interval $0 \leqslant \xi \leqslant 1$, and further using the orthogonal relations of Eq. (12), the undetermined coefficients $p_m (m = 1,2,\ldots)$ can be obtained. The uncoupled dimensionless deflection is therefore

$$w^* = \sum_{m=1}^{\infty} \frac{-R_m q^* \varphi_m}{(\omega_m^2 - \omega_0^2\Omega^2)(\mathrm{e}^{2r_2}+1)}, \tag{20}$$

where $R_m = B_3\int_0^1 \varphi_m(\mathrm{e}^{r_2\xi} + \mathrm{e}^{2r_2}\mathrm{e}^{-r_2\xi})\mathrm{d}\xi$.

Considering the free vibration of the thermal actuator, in which there is no exciting thermal load in $\mathbf{WC} = \mathbf{F}$. In this case, the dimensionless coupled eigenfrequency Ω can be determined by solving the determinant as $|\mathbf{W}| = 0$. The calculated eigenfrequency is expected to be in a complex form, in which the real part $\mathrm{Re}(\Omega)$ gives the new natural frequency and the imaginary part $\mathrm{Im}(\Omega)$ indicates the attenuation of the free vibration. The influence of the thermoelastic effect for each eigenmode can be quantified by the relative resonant frequency shift defined by $\Delta_m = \frac{\mathrm{Re}(\Omega)-\omega_m}{\omega_m}$, and the energy dissipation measured by the quality factor as $Q = 2\left|\frac{\mathrm{Re}(\Omega)}{\mathrm{Im}(\Omega)}\right|$.

4. Results and discussions

We consider a thermal bimorph actuator made of aluminum and polysilicon. Layers 1 and 2 in the above model denote aluminum and polysilicon, respectively. The thermo-mechanical properties of aluminum and polysilicon are listed in Table 1. The dimensions of the beam are $l = 500$ μm, $b = 20$ μm, $h_1 = 2$ μm and $h_2 = 2$ μm, respectively. Since the excitation frequency of the thermal load is within the range of the first few eigenmodes, the infinite system of the eigenmode expansion of w^* can then be truncated as a finite system by selecting only the lowest few eigenmodes. We choose the superposition of the first three eigenmodes and denoted as $w^* = \sum_{n=1}^{3} p_n\varphi_n$. The eigenmodes and the associated natural frequencies for a cantilever beam are already derived by Melrovitch (1986). The first three natural frequencies are $\omega_m = c_m^2\sqrt{\frac{E_c I_c}{m_c l^4}}$ (with

Table 1
Thermo-mechanical properties of bimorph materials used in the simulation

	Aluminum	Polysilicon
Young's modulus (GPa), E	69	150
Poisson's ratio, v	0.334	0.226
Density (kg/m^3), ρ	2692	2330
Coefficient of thermal expansion (1/K), α	23×10^{-6}	2.33×10^{-6}
Thermal conductivity (W/mK), k	235	41
Specific heat (J/kg K), c	900	754

$m = 1,2,3$; $c_1 = 1.875$, $c_2 = 4.694$ and $c_3 = 7.856$). The fundamental frequency of the cantilever beam is chosen as the reference frequency as $\omega_0 = \omega_1$. The first three eigenmodes normalized by Eq. (12b) can be given as

$$\varphi_m = d_m\{[\sin(c_m) - \sinh(c_m)][\sin(c_m\xi) - \sinh(c_m\xi)] + [\cos(c_m) + \cosh(c_m)][\cos(c_m\xi) - \cosh(c_m\xi)]\}, \quad (21)$$

where $d_m = \gamma_m/[\sin(c_m) - \sinh(c_m)]$ (with $m = 1,2,3$; $\gamma_1 = 1.036 \times 10^8$, $\gamma_2 = 1.437 \times 10^8$ and $\gamma_3 = 1.41 \times 10^8$).

Using the first three eigenmodes and the associated natural frequencies, the coupled and uncoupled frequency responses of the temperature and deflection at the free end of the beam can be simulated by solving $\mathbf{WC} = \mathbf{F}$ and directly using Eqs. (19) and (20). The load–deflection and load–temperature responses are plotted in Figs. 2 and 3 respectively for the frequency range of the selected eigenmodes.

The nearly coinciding plots in Figs. 2 and 3 show the weak thermoelastic coupling for the example of aluminum–polysilicon thermal bimorph actuator. It also shows that due to the three pole frequencies in the parametric uncoupled model of Eq. (20), the deflection responses at resonance cannot be simulated. However, the responses around the resonance frequencies can be simulated by using the coupled model, and can be further quantified by first solving $|\mathbf{W}| = 0$ for the complex eigenfrequencies and then calculating the resonant frequency shift and the Q for each eigenmode. The calculated results are listed in Table 2, indicating that the relative resonant frequency shifts are shifted downward in the order of 10^{-3} and the Q's are in the range of 10^3–10^5. Considering the air damping which is considered as a predominant damping source due to the relative large surface area to volume ratio of microstructures, its mechanism can be characterized into three regions, intrinsic, molecular and viscous regions, according to the ambient air pressure (Newell, 1968). Air damping in the intrinsic region is negligible compared to other damping sources such as internal friction and surface effects (Yasumura et al., 2000), whereas in the other two regions it becomes more dominant. In the work of Newell

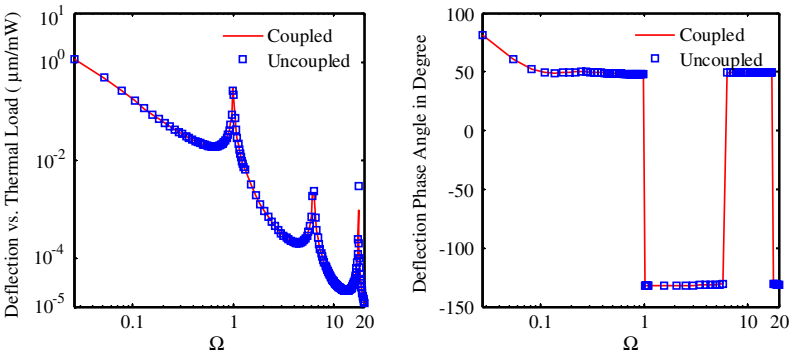

Fig. 2. Amplitude and phase angle of load–deflection frequency response at the free end of the thermal bimorph actuator as a function of dimensionless excitation frequency.

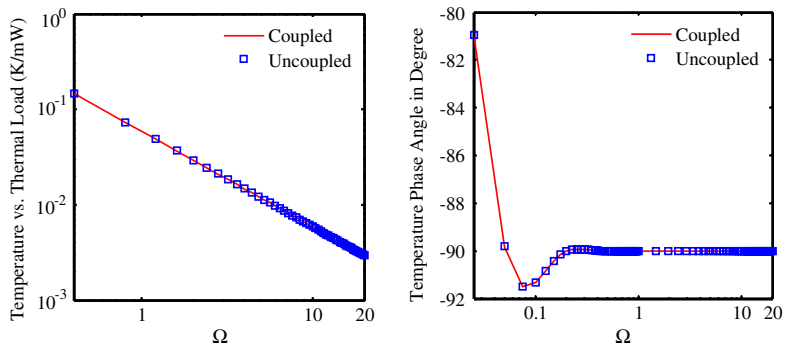

Fig. 3. Amplitude and phase angle of load–temperature frequency response at the free end of the thermal bimorph actuator as a function of dimensionless excitation frequency.

Table 2
Relative resonant frequency shifts and quality factors for each eigenmode in resonance

Mode number	Relative resonant frequency shift	Quality factor
1	-1.5×10^{-3}	6.07×10^{3}
2	-1.2×10^{-3}	3.57×10^{4}
3	-1.3×10^{-3}	1.12×10^{5}

Table 3
Relative resonant frequency shifts and quality factors caused by air damping, and their corresponding ranges of the air pressure P (torr)

	Intrinsic	Molecular	Viscous
Quality factor (Newell, 1968)	$4\times10^{3}(0.1\leqslant P\leqslant 1)$	$4\times10^{3}\leqslant Q\leqslant 2\times10^{2}$ $(1\leqslant P\leqslant 10)$	2×10^{2} $(10\leqslant P\leqslant 10^{5})$
Relative resonant frequency shift (Zhang et al., 2003)	n/a	n/a	$\leqslant10^{-5}$

(1968), the approximate Q's with corresponding air pressure ranges for microstructure with length/thickness = 100 and width = 25 μm, which is geometrically similar to the thermal actuator discussed in this paper, are listed in Table 3. Comparing to the results in Table 2, it indicates that the air damping really is the dominant factor on the Q at a relative low vacuum level ($\geqslant 1$ torr). In the intrinsic region, the Q of air damping is close to that of the fundamental eigenmode. However, the Q of 2×10^{5} for microstructures with different geometries and under the pressure level in the intrinsic region ($\leqslant 7.5\times10^{-3}$ torr) has been observed experimentally (Blom et al., 1992). Therefore, to achieve the high Q performance for a thermal actuator operating in the resonant mode (Schweizer et al., 2000), a proper vacuum encapsulation is needed obviously. The intrinsic vacuum level controlled within is independent of geometry and may be determined empirically (Newell, 1968; Blom et al., 1992). Also following the analytical analysis of the air damping in the viscous region (Zhang et al., 2003), the caused maximum resonant frequency shift is listed in Table 3, indicating that the frequency shift of thermoelastic coupling is more significant than that of air damping. Although the frequency shifts in other pressure regions are not investigated, special attention is still suggested to be paid on this phenomenon for frequency-agile requirement in the sensing application of the thermal bimorph actuator at atmospheric condition (Emmenegger et al., 1998). In the analytical analysis of this paper, it is also worth noting that the dynamic characteristic of thermal actuators is dominated by the first-order characteristic of the heat conduction. This explains the decreasing magnitude in the calculated result of load–deflection shown in Fig. 3 as the driving frequency increases.

5. Conclusions

A dynamic coupled model for a thermal bimorph actuator has been developed and described in this paper. The frequency responses under a harmonically varying thermal load are simulated using the method of eigenmode expansion. For a typical example of an aluminum–polysilicon thermal bimorph actuator, the effects of thermoelastic coupling on the resonant frequencies and the Q's are studied and compared to the effects of air damping. It shows that the resonant frequencies due to the thermoelastic coupling are generally shifted downward with the order larger than that of air damping. Also only under high vacuum level, the influence of thermoelastic coupling on the Q could be more significant than that of air damping. Thus a proper vacuum encapsulation is needed for the high Q requirement of the thermal actuator in the resonant mode. Based on this theoretical model, the thermo-mechanical behavior of a thermal actuator is investigated, and the obtained results provide insights which enable and facilitate further optimization of the dynamic characteristics of thermal actuators.

References

Blom, F.R., Bouwstra, S., Elwenspoek, M., Fluitman, J.H.J., 1992. Dependence of the quality factor of micromachined silicon beam resonators on pressure and geometry. J. Vac. Sci. Technol. B 10, 19–26.

Boley, B.A., Weiner, J.H., 1960. Theory of thermal stresses. Wiley, New York.
Emmenegger, M., Taschini, S., Korvink, J.G., Baltes, H., 1998. Simulation of a thermomechanically actuated gas sensor. In: Proc. of the IEEE MEMS'98 Heidelberg, Germany, 184–189.
Fung, Y.C., 1965. Foundations of solid mechanics. Prentice-Hall, Englewood Cliffs, New Jersey.
Geisberger, A.A., Sarkar, N., Ellis, M., Skidmore, G.D., 2003. Electrothermal properties and modeling of polysilicon microthermal actuators. J. Microelectromech. Syst. 12 (4), 513–522.
Hickey, R., Sameoto, D., Hubbard, T., Kujath, M., 2003. Time and frequency response of two-arm micromachined thermal actuators. J. Micromech. Microeng. 13, 40–46.
Mankame, N.D., Ananthasuresh, G.K., 2001. Comprehensive thermal modelling and characterization of an electro-thermal-compliant microactuator. J. Micromech. Microeng. 11, 452–462.
Melrovitch, L., 1986. Elements of vibration analysis, 2nd ed. McGraw-Hill, New York.
Newell, W.E., 1968. Miniaturization of tuning forks. Science 161, 1320–1326.
Roszhart, T.V., 1990. The effect of thermoelastic internal fiction of the Q of micromachined silicon resonator. In: Proc. of the solid-state sensor and actuator workshop, Hilton Head Island, SC, 13–16.
Schweizer, S., Cousseau, P., Lammel, G., Calmes, S., Renaud, P., 2000. Two-dimensional thermally actuated optical microprojector. Sens. Actuators. A 85, 424–429.
Yasumura, K.Y., Stowe, T.D., Chow, E.W., Pfafman, T., Kenny, T.W., Stipe, B.C., Rugar, D., 2000. Quality factors in micro- and submicron-thick cantilevers. J. Microelectromech. Syst. 9 (1), 117–125.
Zener, C., 1937. Internal fiction in solids I. theory of internal fiction in reeds. Phys. Rev. 52, 230–235.
Zener, C., 1938. Internal fiction in solids II. general theory of thermoelastic internal fiction. Phys. Rev. 53, 90–99.
Zhang, C., Xu, G., Jiang, Q., 2003. Analysis of the air-damping effect on a micromachined beam resonator. Math. Mech. Solids 8 (3), 315–325.